Quantum theory of SASE FEL

R. Bonifacio[a], N. Piovella[a], G.R.M. Robb[b]

[a] *Dipartimento di Fisica, Università Degli Studi di Milano,*

INFM and INFN, Via Celoria 16, I-20133 Milano, Italy.

[b] *Department of Physics, University of Strathclyde, Glasgow, G4 0NG, Scotland.*

Abstract

We describe a free-electron laser (FEL) in the Self Amplified Spontaneous Emission (SASE) regime quantizing the electron motion and taking into account propagation effects. We demonstrate quantum purification of the SASE spectrum, i.e., in a properly defined quantum regime the spiking behavior disappears and the SASE power spectrum becomes very narrow.

PACS numbers: 41.60.Cr,42.50.Fx

The Self Amplified Spontaneous emission (SASE) regime for a free-electron laser (FEL) is made up of three basic ingredients: high-gain, propagation or "slippage" effects and start-up from noise [1]. The classical steady-state high-gain regime of FELs, with universal scaling and the introduction of the ρ-BPN parameter, was analysed in ref.[2], where the possibility of operating an FEL in the SASE regime was described. The first experimental observation of the high-gain regime, also starting from noise, was carried out in the microwave range using a waveguide in the Livermore experiment [3]. Presently, short wavelength FELs which amplify incoherent shot noise via SASE are of great interest worldwide as potential sources of ultra bright coherent X-ray radiation [4, 5].

Many theoretical studies of high-gain FELs [6] do not take into account propagation effects and the initial noise is described by a small input signal or a small bunching. Other treatments assume that SASE is just steady-state amplification starting from noise, ignoring propagation effects [7, 8]. That approach does not give the correct temporal structure and spectrum of the SASE radiation as described in ref. [1].

In ref. [9, 10] it was shown that due to propagation there exists not only the steady-state instability of ref. [2], but also a superradiant instability, with peak intensity proportional to n^2, where n is the electron density. This instability originates in the region near the rear edge of the electron bunch, producing a soliton-like pulse which grows and narrows as it slips over the electrons, preserving a hyperbolic secant shape with some ringing [11]. We stress that the mathematics and the physics of this superradiant instability, which is at the heart of SASE [1], is completely different from the usual steady-state instability. A striking example of the difference between the steady-state and superradiant regimes is that superradiantly amplified spikes occur when the system is detuned from resonance, whereas the steady-state instability does not occur [9, 10]. In this case, the superradiant instability is actually stronger than for the case of exact resonance, since the radiation pulse propagates over fresh electrons, which have not been perturbed by the steady-state instability.

As shown in ref. [1], a SASE FEL radiates a random series of spikes since, roughly speaking, the electron bunch contains many cooperation lengths L_c which radiate randomly and independently from one another. The final result is an almost chaotic temporal pulse structure with a broad spectral width. The number of spikes in the high-gain regime corresponds approximately to the number of cooperation lengths in the electron bunch. Only when the length of the electron bunch is a few cooperation lengths is a partial "cleaning"

of the temporal profile of the radiation obtained, as described in ref. [1]. Furthermore, the total radiated energy does not behave as that predicted by steady-state theory. After reaching the steady-state value of saturation, the energy for SASE continues to increase due to the fact that the superradiant spikes do not saturate. However, SASE has one drawback with regard to its application as a useful source of short-wavelength coherent light : at short wavelengths many cooperation lengths L_c lie within the electron bunch. This implies a quasi-chaotic temporal structure of the radiation pulse and a consequent wide spectrum.

Several schemes have been proposed in order to avoid the large spectral width associated with classical SASE. One of these involves a multiple wiggler scheme with a coherent seed laser [12, 13]. This method is based on the fact that the FEL interaction creates a strong bunching not only on the fundamental but also on the higher harmonics (even and odd), as shown analytically in [12, 14]. Hence, if the electron beam is injected in a second wiggler tuned to one of the higher harmonics, even or odd, the system starts radiating with intensity $\propto n^2$. This superradiant harmonic generation (SRHG) eventually evolves into the high-gain exponential regime. A difficulty in producing SRHG is that "it is necessary to make the first wiggler section long enough to bring the harmonic bunching well above noise, but not so long as to induce too much energy spread" [13]. This optimization of SRHG, termed high-gain harmonic generation (HGHG), has recently been performed by other authors [15]. However, this method presents difficulties when going to very short wavelengths, as pointed out in ref. [16], due to the fact that each stage amplifies not only the coherent signal but also the noise.

In this letter we propose a novel method for producing coherent short wavelength radiation with SASE. We introduce a quantum description of SASE which depends on a dimensionless quantum FEL parameter, $\bar{\rho}$, which determines the number of photons per electron and/or the electron recoil in units of the photon momentum. We show that when $\bar{\rho} \gg 1$ the SASE FEL behaves classically, i.e. in agreement with the SASE classical model. However, when $\bar{\rho} \leq 1$ we obtain a quantum regime with features completely different from those of the classical regime, and which we shall refer as Quantum SASE. A surprising feature of this regime is the phenomenon of "quantum purification", in which the random spiking behavior almost disappears and a strong narrowing of the spectrum occurs. Here we generalize a previous model [17] including propagation effects via a multiple scaling method used in the classical FEL theory of ref. [18]. This allows us to easily take into account the existence of

two different spatial scales in the FEL: the variation of the electron distribution on the scale of the radiation wavelength (describing the bunching) and the variation of the field envelope on the much longer scale of the cooperation length.

The quantum FEL is described by the following equations for the dimensionless radiation amplitude $A(\bar{z}, z_1)$ and the matter wave field $\Psi(\theta, \bar{z}, z_1)$:

$$i\frac{\partial \Psi(\theta,\bar{z},z_1)}{\partial \bar{z}} = -\frac{1}{2\bar{\rho}}\frac{\partial^2}{\partial\theta^2}\Psi(\theta,\bar{z},z_1) - i\bar{\rho}\left[A(\bar{z},z_1)e^{i\theta} - \text{c.c.}\right]\Psi(\theta,\bar{z},z_1) \quad (1)$$

$$\frac{\partial A(\bar{z},z_1)}{\partial \bar{z}} + \frac{\partial A(\bar{z},z_1)}{\partial z_1} = \frac{1}{2\pi}\int_0^{2\pi} d\theta |\Psi(\theta,\bar{z},z_1)|^2 e^{-i\theta} + i\bar{\delta}A(\bar{z},z_1). \quad (2)$$

These equations were derived in detail in ref.[17], to describe Collective Recoil Lasing (CRL) in FELs and in atomic systems. In the CRL equations, the electrons are described by a Schrödinger equation for a matter-wave field Ψ [19, 20] in a self-consistent pendulum potential proportional to A, where $|A|^2 = |a|^2/(N\bar{\rho})$, $|a|^2$ is the average number of photons in the interaction volume V, and $|\Psi|^2$ is the space-time dependent electron density, normalized to unity. In Eqs. (1) and (2) we have adopted the universal scaling used in the classical FEL theory [1, 2, 10], *i.e.* $\theta = (k + k_w)z - ckt$ is the electron phase, where $k_w = 2\pi/\lambda_w$ and $k = \omega/c = 2\pi/\lambda$ are the wiggler and radiation wavenumbers, $\bar{z} = z/L_g$ is the dimensionless wiggler length, $L_g = \lambda_w/4\pi\rho$ is the gain length, $z_1 = (z - v_r t)/\beta_r L_c$ is the coordinate along the electron bunch moving at the resonant velocity $v_r = c\beta_r = ck/(k+k_w)$ and $L_c = \lambda/4\pi\rho$ is the cooperation length or coherence length, $\rho = \gamma_r^{-1}(a_w/4ck_w)^{2/3}(e^2n/m\epsilon_0)^{1/3}$ is the classical BPN parameter [2], $\gamma_r = \sqrt{(\lambda/2\lambda_w)(1+a_w^2)}$ is the resonant energy in mc^2 units, a_w is the wiggler parameter and n is the electron density. Finally, $\bar{p} = (\gamma - \gamma_0)/\rho\gamma_0$ is the dimensionless electron momentum and $\bar{\delta} = (\gamma_0 - \gamma_r)/\rho\gamma_0$ is the detuning parameter, where $\gamma_0 \approx \gamma_r$ is the initial electron energy in mc^2 units. It can be easily shown that Eq. (1) implies:

$$\frac{\partial}{\partial \bar{z}}\int_0^{2\pi} d\theta\, |\Psi(\theta, z_1, \bar{z})|^2 = 0. \quad (3)$$

Hence, the dimensionless density profile $I_0(z_1) = \int_0^{2\pi} d\theta |\Psi|^2$ is independent of $\bar{z}$. This means that the spatial distribution of the particles does not change appreciably on the slow scale z_1 during the interaction with the radiation.

Whereas the classical FEL equations in the above universal scaling do not contain any explicit parameter (see ref. [9, 10]), the quantum FEL equations (1) and (2) depend on the quantum FEL parameter

$$\bar{\rho} = \left(\frac{mc\gamma_r}{\hbar k}\right)\rho. \quad (4)$$

From the definition of A, it follows that $\bar{\rho}|A|^2 = |a|^2/N$ is the average number of photons emitted per electron. Hence, since in the classical steady-state high-gain FEL A reaches a maximum value of the order of unity, $\bar{\rho}$ represents the maximum number of photons emitted per electron, and the classical regime occurs for $\bar{\rho} \gg 1$. Note also that in Eq. (1) $\bar{\rho}$ appears as a "mass" term, so one expects a classical limit when the mass is large. As we shall see, when $\bar{\rho} < 1$ the dynamical behavior of the system changes substantially from a classical to a quantum regime.

A further inspection of Eq. (1) shows that Ψ depends explicitly on θ, which describes the variation (bunching) on the scale of the radiation wavelength λ. The parametrical dependence on z_1 is induced by the slow spatio-temporal evolution of the field amplitude A. This evolution is described by Eq. (2), in which the bunching factor is the ensemble average of $e^{-i\theta}$. In other words, the N-particle system is described as a quantum ensemble represented by the matter-wave field Ψ. This model has been used previously to describe the quantum regime of an FEL [19] and of the Collective Atomic Recoil Laser (CARL) [21, 22, 23, 24, 25, 26], neglecting the dependence on z_1, i.e., propagation. This is appropriate for the FEL when slippage due to the difference between the light and electron velocities is neglected, which is never true in the SASE regime where the propagation from one cooperation length to another is fundamental.

The classical limit of the FEL can be explicitly shown as follows. Eq.(1) can be transformed into an equation for the Wigner function, as shown in ref. [20]:

$$\frac{\partial W(\theta,\bar{p},z_1,\bar{z})}{\partial \bar{z}} + \bar{p}\frac{\partial W(\theta,\bar{p},z_1,\bar{z})}{\partial \theta} - \bar{\rho}\left(Ae^{i\theta} + A^* e^{-i\theta}\right)\left[W\left(\theta,\bar{p}+\frac{1}{2\bar{\rho}},z_1,\bar{z}\right) - W\left(\theta,\bar{p}-\frac{1}{2\bar{\rho}},z_1,\bar{z}\right)\right] = 0, \tag{5}$$

whereas Eq.(2) becomes

$$\frac{\partial A}{\partial \bar{z}} + \frac{\partial A}{\partial z_1} = \frac{1}{2\pi}\int_{-\infty}^{+\infty} d\bar{p}\int_0^{2\pi} d\theta\, W(\theta,\bar{p},z_1,\bar{z})e^{-i\theta} + i\bar{\delta}A. \tag{6}$$

In the right hand side of Eq. (5), the incremental ratio $\bar{\rho}[W(\theta,\bar{p}+1/2\bar{\rho},z_1,\bar{z}) - W(\theta,\bar{p}-1/2\bar{\rho},z_1,\bar{z})] \to \partial W(\theta,\bar{p},z_1,\bar{z})/\partial\bar{p}$ when $\bar{\rho} \to \infty$. Hence, for large values of $\bar{\rho}$, Eq. (5) becomes the Vlasov equation:

$$\frac{\partial W(\theta,\bar{p},z_1,\bar{z})}{\partial \bar{z}} + \bar{p}\frac{\partial W(\theta,\bar{p},z_1,\bar{z})}{\partial \theta} - \left(Ae^{i\theta} + A^* e^{-i\theta}\right)\frac{\partial W(\theta,\bar{p},z_1,\bar{z})}{\partial \bar{p}} = 0. \tag{7}$$

Eqs. (5) and (6) provide the description of the CRL model in terms of the Wigner function for the electrons, whereas Eqs. (6) and (7) are equivalent to the classical FEL model of

ref. [18]. Note that Eqs. (6) and (7) do not depend explicitly on $\bar{\rho}$, as must be the case in the classical model with universal scaling [9, 10]. We briefly mention that Eq. (5) for the Wigner function has a broader validity than the Schrödinger equation (1), since it can also describe a statistical mixture of states which cannot be represented by a wave function but rather by a density operator.

Eqs.(1) and (2) are conveniently solved in the momentum representation. Assuming that $\Psi(\theta, z_1, \bar{z})$ is a periodic function of θ, it can be expanded in a Fourier series:

$$\Psi(\theta, z_1, \bar{z}) = \sum_{n=-\infty}^{\infty} c_n(z_1, \bar{z}) e^{in\theta} \tag{8}$$

so inserting Eq. (8) into Eqs. (1) and (2), we obtain

$$\frac{\partial c_n}{\partial \bar{z}} = -\frac{in^2}{2\bar{\rho}} c_n - \bar{\rho}\left(A c_{n-1} - A^* c_{n+1}\right) \tag{9}$$

$$\frac{\partial A}{\partial \bar{z}} + \frac{\partial A}{\partial z_1} = \sum_{n=-\infty}^{\infty} c_n c_{n-1}^* + i\bar{\delta} A, \tag{10}$$

Eqs. (9) and (10) are our working equations and their numerical analysis will be discussed in the following. Note that from Eq. (8) it follows that $|c_n|^2$ is the probability that an electron has a dimensionless momentum $\bar{p} = n/\bar{\rho}$ (i.e. $mc(\gamma - \gamma_0) = (\hbar k)n$),

$$b = \sum_{n=-\infty}^{\infty} c_n c_{n-1}^* \tag{11}$$

is the quantum expression of the bunching parameter and

$$\langle \bar{p} \rangle = \frac{1}{\bar{\rho}} \sum_{n=-\infty}^{\infty} n |c_n|^2 \tag{12}$$

is the average dimensionless momentum. Note that the quantum bunching (11) requires a coherent superposition of different momentum states. The stability analysis of Eqs. (9) and (10) has been carried out in ref. [24, 25, 26] for the case with no propagation. We assume that the system is in an equilibrium state with no field, $A = 0$, and all the electrons are in the state $n = 0$, with $c_0 = 1$ and $c_m = 0$ for all $m \neq 0$. This equilibrium state is unstable when the dispersion relation

$$(\lambda - \bar{\delta})\left(\lambda^2 - \frac{1}{4\bar{\rho}^2}\right) + 1 = 0, \tag{13}$$

has complex roots. Notice that this dispersion relation coincides with that of a classical FEL with an initial energy spread with a square distribution and width $1/\bar{\rho}$ [10], i.e., this

extra term represents the intrinsic quantum momentum spread which, in dimensional units, becomes $\hbar k$. In fig.1 we plot the imaginary part of λ as a function of $\bar{\delta}$ for different values of $\bar{\rho}$. The classical limit is obtained for $\bar{\rho} \gg 1$ (see fig.1a). In this case, the system is unstable for $\bar{\delta} \lesssim 2$, with maximum instability rate $\mathrm{Im}\lambda = \sqrt{3}/2$ at $\bar{\delta} = 0$. When $\bar{\rho}$ is smaller than unity (fig.1c-f), the instability rate decreases and the peak of $\mathrm{Im}(\lambda)$ moves around $\bar{\delta} = 1/2\bar{\rho}$ (*i.e.* $mc(\gamma_0 - \gamma_r) = \hbar k/2$) with peak value $\mathrm{Im}\lambda = \sqrt{\bar{\rho}}$ and full width on $\bar{\delta}$ equal to $4\bar{\rho}^{1/2}$ (i.e. $mc\Delta\gamma = 4(\hbar k)\bar{\rho}^{3/2}$). As discussed in ref. [25, 26], for $\bar{\rho} \gg 1$ the electrons have almost the same probability of transition from the momentum state $n = 0$ to $n = 1$ or $n = -1$ (i.e. $|c_1|^2 \sim |c_{-1}|^2$), absorbing or emitting a photon. On the contrary, in the case $\bar{\rho} \leq 1$, $|c_1|^2 \ll |c_{-1}|^2$, i.e. the particles can only emit a photon without absorption.

As shown by the linear stability analysis discussed above, the quantum regime occurs for small value of $\bar{\rho}$, when an electron emits only a single photon. In this limit, the dynamics of the interaction is that of a system with only two momentum states, i.e. the initially occupied state with $n = 0$ and the recoiling state with $n = -1$. In this limit, Eq. (9) and (10), after defining the "polarization" $S = c_0 c_{-1}^* \exp[i\bar{\delta}\bar{z}]$ and the "population difference" $D = |c_0|^2 - |c_{-1}|^2$, reduce to the so-called "Maxwell-Bloch equations" for a two-state system [27]:

$$\frac{\partial}{\partial \bar{z}} S(z_1, \bar{z}) = -i\Delta S(z_1, \bar{z}) + \bar{\rho}\bar{A}(z_1, \bar{z}) D(z_1, \bar{z}) \tag{14}$$

$$\frac{\partial}{\partial \bar{z}} D(z_1, \bar{z}) = -2\bar{\rho}\left[\bar{A}(z_1, \bar{z})^* S(z_1, \bar{z}) + \text{c.c.}\right] \tag{15}$$

$$\frac{\partial \bar{A}}{\partial \bar{z}} + \frac{\partial \bar{A}}{\partial z_1} = S(z_1, \bar{z}). \tag{16}$$

where $\Delta = \bar{\delta} - 1/2\bar{\rho}$ and $\bar{A} = A \exp(-i\bar{\delta}\bar{z})$. Notice that the parameter $\bar{\rho}$ in Eqs. (14)-(16) may be eliminated by redefining the variables as $A' = \sqrt{\bar{\rho}}\bar{A}$, $z' = \sqrt{\bar{\rho}}\bar{z}$, $z_1' = \sqrt{\bar{\rho}} z_1$ and $\Delta' = \Delta/\sqrt{\bar{\rho}}$. With this quantum universal scaling the cooperation length becomes $L_c' = L_c/\sqrt{\bar{\rho}} \propto 1/\sqrt{n}$. An interesting result of this scaling is that the CRL model of Eqs. (1) and (2) can now be interpreted as a Schrödinger equation for a single particle with a "mass" $\bar{\rho}^{3/2}$ in a self-consistent pendulum potential. This provides an intuitive interpretation of the classical limit which holds when the particle's "mass" is large.

We now discuss some analytical results arising from the quantum SASE model. It has been shown in a previous work [17] that the classical model of Eqs. (6) and (7) admits a soliton-like self-similar solution $A(\bar{z}, z_1) = z_1 A_1(y)$ when $\bar{\delta} = 0$, where $y = \sqrt{z_1}(\bar{z} - z_1) \approx$

$(z-v_r t)^{1/2}(ct-z)/L_c^{3/2}$ (where we have assumed $\beta_r \sim 1$) [11]. This means that the radiation pulse propagates over the electron bunch (i.e. at different values of z_1), preserving its shape but increasing with amplitude $\propto z_1$ and narrowing with width $\propto 1/\sqrt{z_1}$. It is possible to show [10] that in the linear regime the radiation pulse has a maximum at $z_1 = \bar{z}/3$ and propagates at a constant velocity $v_s = 3v_r/(2+\beta_r)$.

An analogous self-similar solution also exists for the quantum equations (14)-(16) when $\Delta = 0$ [28], i.e. $A(\bar{z}, z_1) = z_1 A_2(x)$, where $x = \bar{\rho} z_1(\bar{z} - z_1) = (z - v_r t)(ct - z)/L_c'^2$ (with $L_c' = L_c/\sqrt{\bar{\rho}}$). The shape of the radiation pulse is similar in the classical and quantum cases, but in the quantum case its width decreases as $1/\bar{\rho} z_1$. In this case, the radiation pulse in the linear regime has a maximum at $z_1 = \bar{z}/2$ and moves at the constant velocity $v_s = 2v_r/(1+\beta_r)$.

From the features of the self-similar solutions we can deduce some important aspects of the nature of the random spikes emitted in the SASE regime. First, both in the classical and in the quantum regime the dimensionless amplitude A of the field is proportional to $z_1 \propto \rho \propto N^{1/3}$, so that the number of emitted photons $|a|^2 = N\bar{\rho}|A|^2 \propto N^2$, ie. is superradiant. Whereas the characteristic spatial length in the classical regime is L_c, in the quantum regime the characteristic length is $L_c' = L_c/\sqrt{\bar{\rho}} \gg L_c$ for $\bar{\rho} \ll 1$.

Let us now briefly restate the reasons for the classical random spiking behavior. If the bunch length contains many cooperation lengths L_c, each of them radiates a superradiant spike independently as the electron bunch propagates into the wiggler. Each spike is only roughly represented by a self-similar solution because the radiation from one portion does not find fresh electrons but electrons which have already interacted with radiation. As discussed in [1] the number of spikes increases with the number of cooperation length in the bunch, i.e. $L_b/2\pi L_c$.

We now describe the numerical solution of Eqs.(1) and (2) which demonstrates the different dynamical behavior in the classical and quantum SASE regimes. The SASE simulation has been performed assuming all the electrons are initially in the $n = 0$ momentum state and that there is a weak randomly fluctuating modulation in the electron density along the electron pulse, as is appropriate to model random electron shot noise. The initial conditions for all the simulations are therefore $A(z_1, \bar{z} = 0) = 0$, $c_{-1}(z_1, \bar{z} = 0) = b_0 e^{i\phi(z_1)}$ and $c_0(z_1, \bar{z} = 0) = \sqrt{1 - b_0^2}$, where $b_0 = 0.01$ and $\phi(z_1)$ is a randomly fluctuating phase with values in the range $[0, 2\pi)$. Since there is not a radiation seed, we assume $\bar{\delta} = 0$.

Fig.2 shows the numerical solution for $L_b = 30L_c$ and $\bar{z} = 50$ for the classical regime ($\bar{\rho} = 5$, left column) and the quantum regime ($\bar{\rho} = 0.05$, right column). Figures 2a and 2b show the intensity $|A|^2$ as a function of the dimensionless variable z_1 (i.e. the coordinate along the electron bunch in units of L_c in the electron rest frame), whereas figures 2c and 2d show the power spectrum $P(\bar{\omega})$ as a function of $\bar{\omega} = (L_c/c)(\omega' - \omega)$, where ω' is the field frequency and ω is the carrier resonant frequency. In fig. 2a and 2b , $z_1 = 0$ is the trailing edge and $z_1 = 30$ is the leading edge of the electron bunch. Therefore, the region on the left of the dotted line is the radiation on the electron beam, on the right is free propagation in vacuum.

Alternatively one can interpret fig. 2a and 2b as the temporal behavior of the intensity for an observer which is at a given position in the wiggler and which will see the pulse as it appears from right to left in the figure. We stress that in the classical theory with universal scaling the two cases should be identical. On the contrary, the dramatic difference is evident from fig. 2: the temporal structure in the classical limit (fig. 2a) is almost chaotic and the width of the spectrum is large (fig. 2c). Conversely, the temporal behavior in the quantum limit (fig. 2b) shows a purification of the initially noisy evolution so that the temporal structure looks similar to the self similar solution one would obtain with a coherent seed signal. The corresponding spectrum becomes extremely narrow (fig. 2d), much sharper than the classical one. It can be seen in fig. 2d that the frequency is shifted by $1/2\bar{\rho} = 10$, in agreement with the predictions of the linear analysis described earlier (see fig. 1). The behaviour of the system is similar to what would be expected if the quantum cooperation length is much larger than the classical cooperation length, so that all electrons radiate coherently in the quantum regime. The difference between classical and quantum SASE behavior is confirmed by a comparison of fig. 3a and 3b, which show the total radiated energy, E (in units of $|A|^2$), in the classical and quantum regimes respectively, where

$$E = \int_0^{\bar{z}+\bar{L}} |A|^2 dz_1.$$

In the quantum regime we observe a behavior similar to that which one would obtain with a coherent seed signal in the long bunch superradiant case [9, 10].

Finally, we discuss the reason for quantum purification of the spectrum. As remarked earlier, in fig 1 the gain bandwidth (which is the reciprocal of the "real" coherence length) decreases as $\bar{\rho}^{3/2}$ in the quantum regime. Note that the cooperation length in the quantum

regime, $L_c' = L_c/\sqrt{\bar{\rho}}$, has the same dependence on $\bar{\rho}$. Hence, one can understand that in quantum SASE, i.e., for small value of $\bar{\rho}$, the system behaves as if the startup of the FEL interaction is initiated by a coherent bunching or coherent seed.

In conclusion, in this letter we have given a proof of principle of the novel regime of Quantum SASE, with dynamical properties very different from "normal" classical SASE. In particular, quantum SASE predicts quantum purification of the temporal structure and spectrum. The possibility of experimental observation of this quantum regime is under investigation and will be discussed elsewhere.

We acknowledge useful discussions with S. Bertolucci, L. Serafini, M. Ferrario and L. Palumbo. This work is supported by INFN.

---

[1] R. Bonifacio, L. De Salvo, P. Pierini, N. Piovella, and C. Pellegrini, Phys. Rev. Lett. 73 (1994) 70.

[2] R. Bonifacio, C. Pellegrini and L, Narducci, Opt. Commun. 50 (1984) 373.

[3] T.J. Orzechowski et al., Phys. Rev. Lett. 54 (1985) 889.

[4] J. Andruszkow *et al.*, Phys. Rev. Lett. 85 (2000) 3825.

[5] S.V. Milton *et al.*, Science 292 (2001) 2037.

[6] N.M. Kroll and W.A. McMullin, Phys. Rev. A 17 (1978) 300; I.B. Bernstein and J.H. Hirschfield, Phys. Rev. A 20 (1979) 1661; A.M. Kondratenko, and E.L. Saldin, part. Accel. 10 (1980) 207; V.N. Baier and A.I. Mil'shtein, Sov. Phys. Dokl. 25 (1980) 112; A. Grover and P. Sprangle, IEEE J. Quantum Electron., QE-17 (1981) 1196.

[7] K.J.Kim, Phys. Rev. Lett. 57 (1986) 1871.

[8] J.M. Wang and L.H. Yu, Nucl. Instrum. Meth. A 250 (1986) 396.

[9] R. Bonifacio, B. W. J. McNeil, and P. Pierini, Phys. Rev. A 40 (1989) 4467.

[10] R. Bonifacio, F. Casagrande, G. Cerchioni, L. De Salvo Souza, P. Pierini & N. Piovella, Rivista del Nuovo Cimento 13, No. 9 (1990).

[11] R. Bonifacio, C. Maroli and N. Piovella, Opt. Commun. 68 (1988) 369.

[12] R. Bonifacio, L. De Salvo, and P. Pierini, Nucl. Instrum. Meth. A 293 (1990) 627.

[13] R. Bonifacio, L. De Salvo, P. Pierini, and E.T. Scharlemann, Nucl. Instrum. Meth. A 296 (1990) 787.

[14] R. Bonifacio, R. Corsini, and P. Pierini, Phys. Rev. A 45 (1992)4091.

[15] L.H. Yu, Phys. Rev. A 44 (1991) 5178.

[16] E.L. Saldin, E.A. Schneidmiller, and M.V. Yurkov, Opt. Commun. 202 (2002) 169.

[17] R. Bonifacio, N. Piovella, G.R.M. Robb, and M.M. Cola, submitted to Opt. Commun.

[18] G.T. Moore and M.O. Scully, Phys. Rev.A 21 (1980) 21.

[19] G. Preparata, Phys. Rev.A 38 (1988) 233.

[20] R. Bonifacio, M. Cola, N. Piovella, and G.R.M. Robb, Europhys. Lett. 69 (2005) 55.

[21] R. Bonifacio, L. De Salvo Souza, Nucl. Instrum. and Meth. in Phys. Res. A 341 (1994) 360.

[22] R. Bonifacio, L. De Salvo Souza, L. Narducci and E.J. D'Angelo, Phys. Rev.A 50 (1994) 1716.

[23] R. Bonifacio and L. De Salvo Souza, Optics Comm. 115 (1995) 505.

[24] M.G. Moore, and P. Meystre, Phys. Rev.A 58 (1998) 3248.

[25] N. Piovella, M. Gatelli and R. Bonifacio, Optics Comm. 194 (2001) 167.

[26] N. Piovella, M. Cola, R. Bonifacio, Phys. Rev.A 67 (2003) 013817.

[27] F.T. Arecchi, and R. Bonifacio, IEEE Quantum Electron. 1 (1965) 169.

[28] D. C. Burnham and R. Y. Chiao, Phys. Rev. 188 (1969) 667.

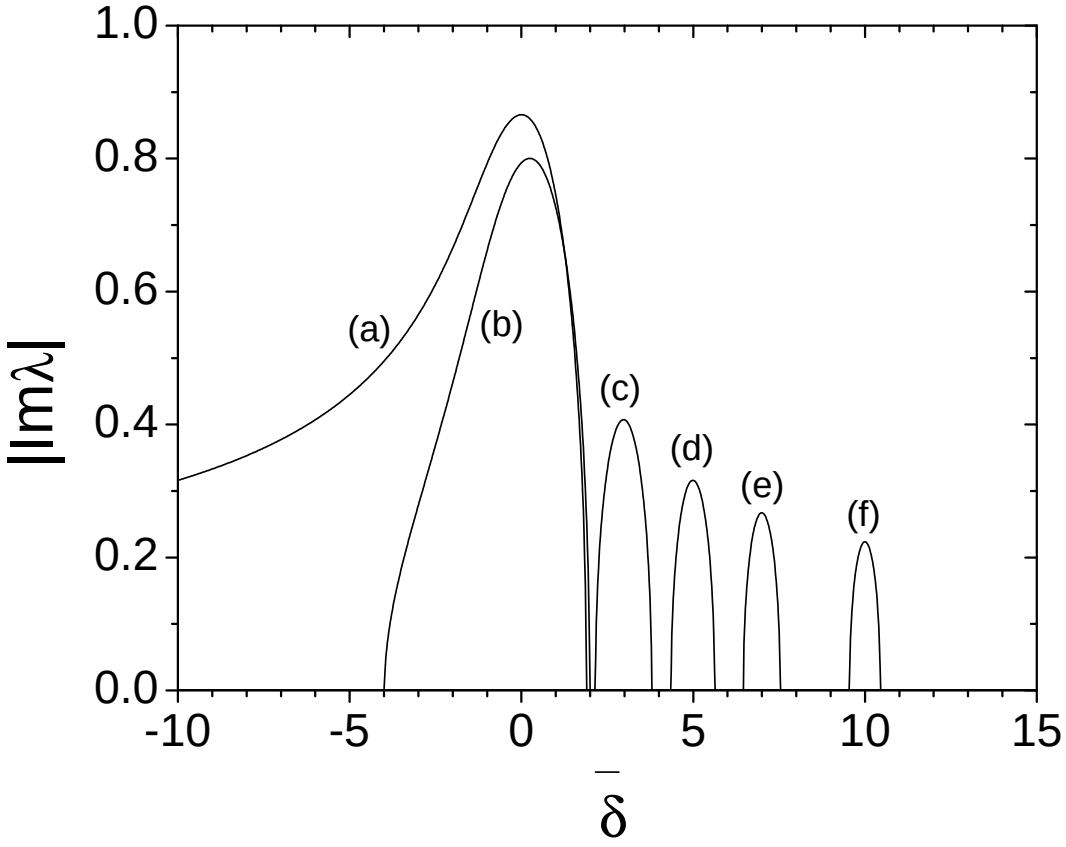

FIG. 1: Imaginary part of the unstable root of the cubic equation (13) vs. $\bar{\delta}$, for $1/2\bar{\rho} = 0$, (a), 0.5, (b), 3, (c), 5, (d), 7, (e) and 10, (f).

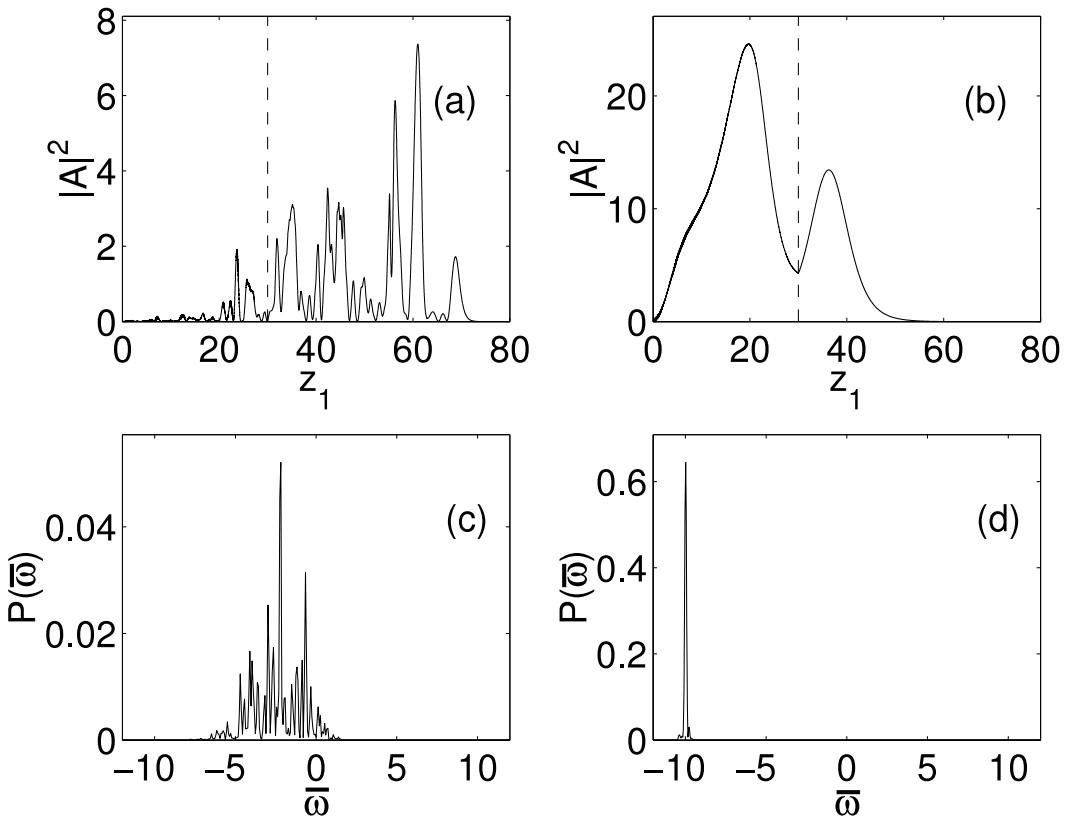

FIG. 2: Numerical solutions of eq. (9) and (10) in the classical and quantum regimes : Graphs (a) and (b) show the scaled intensity $|A|^2(z_1)$ at $\bar{z} = 50$ when the system evolves classically ($\bar{\rho} = 5$) and quantum mechanically ($\bar{\rho} = 0.05$) respectively. Graphs (c) and (d) show the corresponding scaled power spectra $P(\bar{\omega})$ at $\bar{z} = 50$ when $\bar{\rho} = 5$ and $\bar{\rho} = 0.05$ respectively. The frequency shift in (d) is $1/2\bar{\rho} = 10$ in agreement with that predicted from fig. 1. In all cases, $\bar{L} = 30$ and $\delta = 0$ has been used.

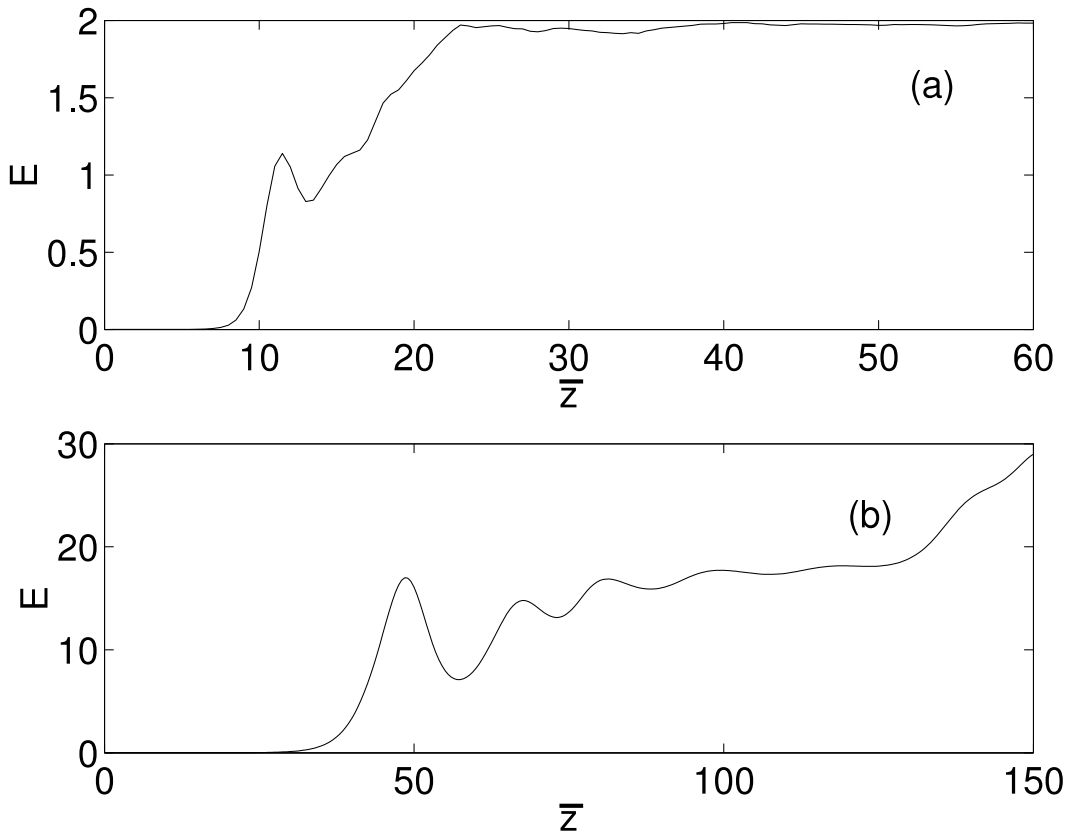

FIG. 3: Scaled energy, E, as a function of $\bar{z}$ when (a) $\bar{\rho} = 5$ and (b) $\bar{\rho} = 0.05$. In both cases $\delta = 0$ and $\bar{L} = 30$.